In-Plane Aromaticity in 1,3-Dipolar Cycloadditions. Solvent Effects, Selectivity, and Nucleus-Independent Chemical Shifts

Fernando P. Cossío,*,† Iñaki Morao,† Haijun Jiao,‡ and Paul von Ragué Schleyer*,‡

Contribution from the Kimika Fakultatea, Euskal Herriko Unibertsitatea, P.K. 1072, San Sebastián-Donostia, Spain, and the Institut für Organische Chemie, Friedrich-Alexander Universität Erlangen-Nürnberg, Henkestrasse 42, D-91054 Erlangen, Germany

Received September 1, 1998. Revised Manuscript Received May 14, 1999

Abstract: The aromaticity and the regiochemistry of several 1,3-dipolar cycloadditions have been studied computationally. It is found that all the transition structures associated with concerted *supra-supra* processes are in-plane aromatic, and this aromaticity is compatible with a ring current circulating along the molecular plane. Solvent effects enhance the activation barrier of the reaction and diminish its synchronicity, with little impact on aromaticity. According to our calculations, aromaticity is important but does not determine the regiochemistry of the reaction. Other phenomena such as electrostatic interactions and solvent effects can modify the regiochemical and the stereochemical outcome.

Introduction

The concept of 1,3-dipolar cycloaddition was defined as a general type of reaction by Huisgen, who developed an impressive research program to explore the preparative possibilities of this reaction, as well as its mechanistic aspects.[1] Nowadays, 1,3-dipolar cycloaddition reactions are one of the best and more general methods for the construction of five-membered rings in a convergent and stereocontrolled manner.[2] Among the 1,3-dipoles involving second-period elements, nitrile oxides[3] and nitrones[4] have proved to be among the most useful and versatile reagents (Scheme 1). The wide range of substituents accessible in the dipolarophiles has allowed the chemical synthesis of a considerable number of nitrogen and oxygen-containing heterocycles, in both inter- and intramolecular processes.[2,5] In addition, such cycloadducts can be transformed further into very attractive compounds by means of well-known procedures.[5c,6]

Scheme 1

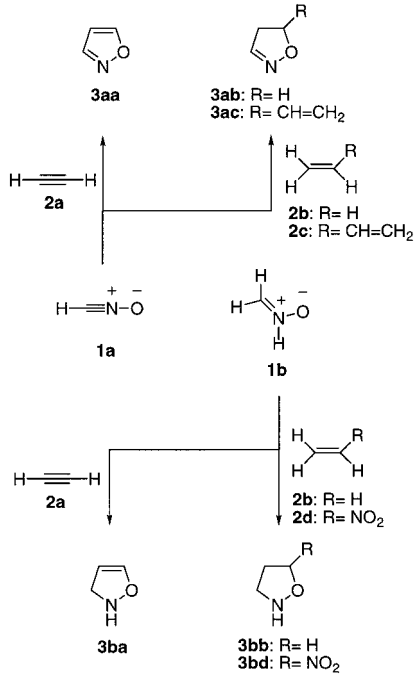

Given the importance of these reactions, an intensive effort has been directed toward the elucidation of its mechanism.[7] The development of the theory of pericyclic reactions led to the rationalization of substituent effects on their regio- and stereoselectivity.[8] These models emerged from the combination of

† Kimika Fakultatea.

‡ Friedrich-Alexander Universität Erlangen-Nürnberg.

(1) (a) Huisgen, R. *Proc. Chem. Soc. (London)* **1961**, 357. (b) Huisgen, R. *Angew. Chem., Int. Ed. Engl.* **1963**, *2*, 565. (c) Huisgen, R. *Angew. Chem., Int. Ed. Engl.* **1963**, *2*, 633. (d) Huisgen, R. In *1,3-Dipolar Cycloaddition Chemistry*; Padwa, A., Ed.; Wiley: New York, 1984; Vol. 1, pp 1−176.

(2) (a) *1,3-Dipolar Cycloaddition Chemistry*; Padwa, A., Ed.; Wiley: New York, 1984; Vols. 1 and 2. (b) Cinquini, M.; Cozzi, F. In *Stereoselective Synthesis*; Helmchen, G., Hoffmann, R. W., Mulzer, J., Schaumam, E., Eds.; GeorgThieme: Stuttgart, 1996; Vol. 5, pp 2953−2987. (c) Padwa, A. In *Comprehensive Organic Synthesis*; Trost, B. M., Fleming I., Eds.; Pergamon: Oxford, 1991; Vol. 4, pp 1069−1109. (d) Wade, P. A. In *Comprehensive Organic Synthesis*; Trost, B. M., Fleming I., Eds.; Pergamon: Oxford, 1991; Vol. 4, pp 1111−1168. (e) Torssell, K. B. G. *Nitrile Oxides, Nitrones and Nitronates in Organic Synthesis*; VCH: New York, 1988. (f) For a recent review on asymmetric 1,3-dipolar reactions, see: Gothelf, K. V.; Jorgensen, K. A. *Chem. Rev.* **1998**, *98*, 863.

(3) (a) Larsen, K. E.; Torssell, K. B. G. *Tetrahedron* **1984**, *40*, 2985. (b) Caramella, P.; Grünanger, P. In *1,3-Dipolar Cycloaddition Chemistry*; Padwa, A., Ed.; Wiley: New York, 1984; Vol. 1, pp 177−290. (c) Kozikowski, A. P. *Acc. Chem. Res.* **1984**, *17*, 410. (d) Easton, C. J.; Merric, C.; Hughes, M.; Savage, G. P.; Simpson, G. W. *Adv. Heterocycl. Chem.* **1994**, *60*, 261.

(4) (a) Black, D. St. C.; Crozier, R. F.; Davies V. C. *Synthesis* **1975**, 205. (b) Confalone, P. N.; Huie, E. M. *Org. React.* **1988**, *36*, 1. (c) Frederickson, M. *Tetrahedron* **1997**, *53*, 403.

(5) (a) Oppolzer, W. *Angew. Chem., Int. Ed. Engl.* **1977**, *16*, 10. (b) Toy, A.; Thompson, W. J. *Tetrahedron Lett.* **1984**, *25*, 3533. (c) Balasubramanian, N. *Org. Prep. Proced. Int.* **1985**, *17*, 23.

(6) (a) Carruthers W. In *Cycloaddition Reactions in Organic Synthesis*; Tetrahedron Organic Chemistry Series; Pergamon Press: Oxford, 1990. (b) Tufariello, J. J. In *1,3-Dipolar Cycloaddition Chemistry*; Padwa, A., Ed.; Wiley: New York, 1984; Vol. 2, pp 83−168. (c) Vasella, A. *Helv. Chim. Acta* **1977**, *60*, 416.

(7) (a) Huisgen, R. *Angew. Chem., Int. Ed. Engl.* **1963**, *2*, 633. (b) Huisgen, R. *J. Org. Chem.* **1968**, *33*, 2291.

10.1021/ja9831397 CCC: $18.00
Published on Web 07/03/1999

Scheme 2[a]

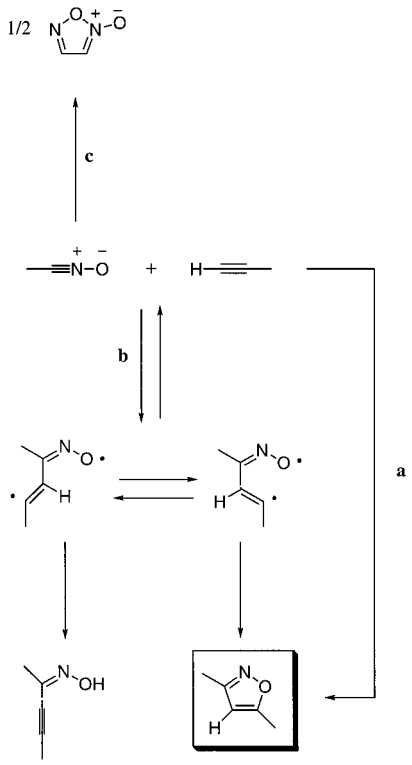

[a] Unless otherwise noted, the substituents at the different positions are not specified.

experimental data and computational studies.[9] However, the nature of the mechanism of 1,3-dipolar cycloadditions was not free from controversy.[1d,10] Thus, the high reactivity of nitrile oxides can yield dimerization products (Scheme 2) or oximes.[11] The latter products can be rationalized in terms of stepwise processes (Scheme 2, path b), which can compete with the concerted reaction (Scheme 2, path a). Alternatively, the product distribution may be governed by the second step of a stepwise mechanism. On the basis of intensive experimental work, Huisgen[1d,6] developed a six-electron *supra-supra* concerted mechanism in accord with the Woodward−Hoffmann rules.[12] This model was confirmed by the pioneering computational studies reported by Leroy and Poppinger.[13] In contrast, Firestone proposed a stepwise mechanism involving biradical intermediates.[14] This mechanism was vigorously criticized by Huisgen.[1d,15] The controversy has long since been resolved. The high stereoselectivity (over 99.997%) observed in one experiment with diazomethane and methyltiglate[16] excludes the presence of diradical intermediates. This result was also obtained within the NMR detection limits in experiments with a nitrile oxide and 1,2-dideuterioethylene (Scheme 3).[17]

Scheme 3[a]

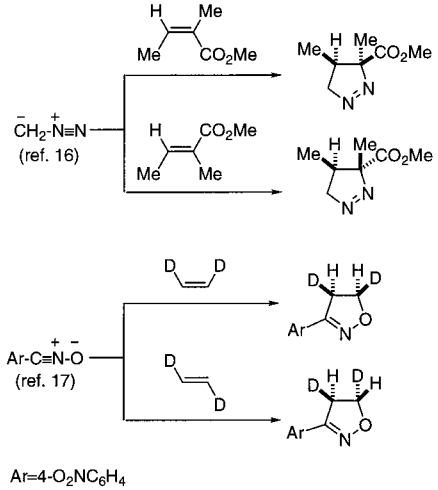

[a] In chiral compounds only one enantiomer is drawn.

Solvent effects in 1,3-dipolar cycloadditions were also extensively studied by Huisgen.[18] This author found a low solvent effect for this reaction, a result that was interpreted in terms of early transition structures,[1d,19] associated with concerted mechanisms.

If [3+2] cycloaddition reactions take place via concerted mechanisms, the corresponding transition structures should be aromatic in character. The idea that thermal pericyclic reactions have aromatic character stems from Evans[20a] and has been supported by Dewar[20b] and Zimmerman.[20c] The connection between the FMO and the aromaticity models is evident if one takes into account that the Woodward−Hoffmann rule for the thermal *supra-supra* cycloadditions is similar to the Hückel rule. However, these considerations do not provide any information about the actual nature of an aromatic transition state. In a previous preliminary paper,[21] we have reported that in 1,3-dipolar cycloadditions the corresponding transition structures are *in-plane* aromatic in character. However, the definition of aromaticity has been problematic[22] and the characterization of *in-plane* aromaticity is even more difficult.[23] In previous papers from our groups, we have evaluated the nucleus-independent

(8) (a) Sustmann, R. *Tetrahedron Lett.* **1971**, 2717. (b) Houk, K. N.; Sims, J.; Watts, C. R.; Luskus, L. *J. Am. Chem. Soc.* **1973**, *95*, 7301. (c) Houk, K. N.; Sims, J.; Duke, R. E.; Strozier, R. W.; George, J. K. *J. Am. Chem. Soc.* **1973**, *95*, 7287. (d) Sustmann, R. *Pure Appl. Chem.* **1974**, *40*, 569. (e) Houk, K. N. *Acc. Chem. Res.* **1975**, *8*, 361. (f) Houk, K. N.; Yamaguchi, K. In *1,3-Dipolar Cycloaddition Chemistry*; Padwa, A., Ed.; Wiley: New York, 1984; Vol. 2, pp 407−450.

(9) See for example: (a) Komornicki, A.; Goddard, J. D.; Schaefer, H. F., III *J. Am. Chem. Soc.* **1980**, *102*, 1763. (b) McDouall, J. J.; Robb, M. A.; Niazi, U.; Bernardi, F.; Schlegel, H. B. *J. Am. Chem. Soc.* **1987**, *109*, 4642. (c) Sosa, C.; Andzelm J.; Lee, C.; Blake, J. F.; Chenard, B. L.; Butler, T. W. *Int. J. Quantum Chem.* **1994**, *49*, 511. (d) Sustmann, R.; Sicking, W.; Huisgen, R. *J. Am. Chem. Soc.* **1995**, *117*, 9679. (e) Annunziata, R.; Benaglia, M.; Cinquini, M.; Cozzi, F.; Raimondi, L. *J. Org. Chem.* **1995**, *60*, 4697. (f) Rastelli, A.; Bagatti, M.; Gandolfi, R. *J. Am. Chem. Soc.* **1995**, *117*, 4965.

(10) Houk, K. N.; Gonzalez, J.; Li, Y. *Acc. Chem. Res.* **1995**, *28*, 81.

(11) Mayr, H.; Baran, J.; Heigl, U. W. *Gazz. Chim. Ital.* **1991**, *121*, 373.

(12) (a) Woodward, R. B.; Hoffmann, R. *J. Am. Chem. Soc.* **1965**, *87*, 395. (b) Woodward, R. B.; Hoffmann, R. *Angew. Chem., Int. Ed. Engl.* **1969**, *8*, 781. (c) Woodward, R. B.; Hoffmann, R. *The Conservation of Orbital Symmetry*; Verlag Chemie: Weinheim, 1970.

(13) (a) Leroy, G.; Nguyen, M.-T.; Sana, M. *Tetrahedron* **1976**, *32*, 1529. (b) Leroy, G.; Nguyen, M.-T.; Sana, M. *Tetrahedron* **1978**, *34*, 2459. (c) Poppinger, D. *J. Am. Chem. Soc.* **1975**, *97*, 7486. (d) Poppinger, D. *Aust. J. Chem.* **1976**, *29*, 465.

(14) (a) Firestone, R. A. *J. Org. Chem.* **1968**, *33*, 2285. (b) Firestone, R. A. *J. Org. Chem.* **1972**, *37*, 2181. (c) Firestone, R. A. *Tetrahedron* **1977**, *33*, 3309.

(15) Huisgen, R. *J. Org. Chem.* **1976**, *41*, 403.

(16) Bihlmaier, W.; Geittner, J.; Huisgen, R.; Reissig, H.-V. *Heterocycles* **1978**, *10*, 147. In an experiment with methyl angelate, the retention of configuration in the dipolarophile was estimated to be >98%. See: Van Auken, T. V.; Rinehart, K. L. *J. Am. Chem. Soc.* **1962**, *84*, 3736.

(17) Houk, K. N.; Firestone, R. A.; Munchausen, L. L.; Mueller, P. H.; Arison, B. H.; Garcia, L. A. *J. Am. Chem. Soc.* **1985**, *107*, 7227.

(18) (a) Geittner, J.; Huisgen, R.; Reissig, H.-V. *Heterocycles* **1978**, *11*, 109. (b) Huisgen, R.; Seidl, H.; Brüning, I. *Chem. Ber.* **1969**, *102*, 1102. (c) Eckell, A.; George, M. V.; Huisgen, R.; Kende, A. S. *Chem. Ber.* **1977**, *110*, 578.

(19) (a) Huisgen, R.; Schug, R. *J. Am. Chem. Soc.* **1976**, *98*, 7819. (b) Huisgen, R. *Pure Appl. Chem.* **1980**, *52*, 2283.

(20) (a) Evans, M. G. *Trans. Faraday Soc.* **1939**, *35*, 824. (b) Dewar, M. J. S. *The Molecular Orbital Theory of Organic Chemistry*; McGraw-Hill: New York, 1969; pp 316−339. (c) Zimmerman, H. *Acc. Chem. Res.* **1971**, *4*, 272.

(21) Morao, I.; Lecea, B.; Cossío, F. P. *J. Org. Chem.* **1997**, *62*, 7033.

chemical shift[24] (NICS) in the center of the reacting systems as well as along the axis perpendicular to the molecular plane as useful methods to characterize *in-plane* aromaticity.[21,25]

The concept of aromaticity of transition states can also be connected with geometric and magnetic parameters,[26] as well as the activation energy.[27] In contrast, the aromaticity of stable molecules has been quantified in terms of aromatic stabilization energy (ASE).[28] On the other hand, the relationship of relevant factors such as regio- and stereoselectivity and aromaticity has not been studied before.

The aim of the present study is to evaluate *in-plane* aromaticity with regard to important variables in chemical reactions such as substituent and solvent effects, to improve knowledge of the factors which determine the energetic parameters of these reactions, as well as the regio- and stereochemistry.

Computational Methods

All the results were obtained with the GAUSSIAN 94 series of programs,[29] using the standard 6-31+G* basis set,[30] chosen to describe properly the significant negative charges present in reactants and transition structures. Electron correlation was partially taken into account by means of density functional theory (DFT)[31] by using the GAUSSIAN 94 version of the hybrid three-parameter functional developed by Becke[32] and denoted as B3LYP. In our preliminary paper, we have found that the B3LYP/6-31+G* results are comparable or even slightly better than those obtained at the MP2(FC)/6-31+G* level.[21] Unless otherwise noted the reported structures have been fully optimized at B3LYP/6-31+G*. The zero-point vibrational energies (ZPVE) were computed at the same level and were not scaled. All stationary points were characterized by harmonic analysis.[33] Nucleus-independent chemical shifts (NICS) were evaluated by using the gauge invariant atomic orbital[34] (GIAO) approach, at the GIAO-SCF/6-31+G*//B3LYP/6-31+G* level. NICS calculations along the intrinsic reaction coordinates[35] (IRC) were performed by employing the sum over states density functional perturbation theory[36] (SOS-DFPT) and a modified version of the deMon-Master program,[37] which incorporates the Pipek-Mezey[38] localization procedure. These calculations used individual gauge for localized orbitals (IGLO) with the IGLO-III TZ2P basis set[39] and the Perdew-Wang-91[40] (PW91) exchange-correlation functional.

Solvent effects were simulated with the self-consistent reaction field method.[41] All the stationary points of the parent systems were optimized by using the Onsager model,[42] which is denoted as the L1A1 method[41d] (multipole expansion truncated at the dipole term, spherical cavity)[43] and the self-consistent isodensity polarization continuum model (SCIPCM),[44] which is considerably more realistic although computationally more demanding. Since the geometries obtained with both approaches were found to be very similar (vide infra), the more complex systems were investigated at the B3LYP(L1A1)/6-31+G*+ZPVE level. Unless otherwise noted, acetonitrile ($\epsilon = 35.94$) was simulated in the SCRF calculations,[45] since this solvent is quite common for this kind of reaction.

The synchronicity[46,47] of the reactions was quantified by using a previously described approach.[48] For a given concerted reaction, "synchronicity" is defined as[49]

$$\mathrm{Sy} = 1 - (2n-2)^{-1}\sum_{i=1}^{n}\frac{|\delta B_i - \delta B_{\mathrm{av}}|}{\delta B_{\mathrm{av}}} \qquad (1)$$

where n is the number of bonds directly involved in the reaction (in this case, $n = 5$) and δB_i stands for the relative variation of a given bond index B_i at the transition structure (TS) relative to the reactants and products, according to the following expression:

(22) (a) Minkin, V. I.; Glukhoutsev, M. N.; Simkin, B. Y. *Aromaticity and Antiaromaticity: Electronic and Structural Aspects*; Wiley: New York, 1994. (b) Minkin, V. I.; Glukhoutsev, M. N.; Simkin, B. Y. *Adv. Heterocycl. Chem.* **1993**, *56*, 303−428. (c) Schleyer, P. v. R.; Jiao, H. *Pure Appl. Chem.* **1996**, *68*, 209 and references therein.

(23) (a) Dewar, M. J. S. *J. Am. Chem. Soc.* **1984**, *106*, 669. (b) Cramer, D. *Tetrahedron* **1988**, *44*, 7427. (c) Schleyer, P. v. R.; Jiao, H.; Glukhovtsev, M. N.; Chandrasekhar, J.; Kraka, E. *J. Am. Chem. Soc.* **1994**, *116*, 10129.

(24) Schleyer, P. v. R.; Maerker, C.; Dransfeld, A.; Jiao, H.; Hommes, N. J. R. v. E. *J. Am. Chem. Soc.* **1996**, *118*, 6317.

(25) Jiao, H.; Schleyer, P. v. R. *J. Phys. Org. Chem.* **1998**, *11*, 655.

(26) Jiao, H.; Schleyer, P. v. R. *Angew. Chem., Int. Ed. Engl.* **1995**, *34*, 334.

(27) (a) Jiao, H.; Schleyer, P. v. R. *J. Chem. Soc., Perkin Trans. 2* **1994**, 407. (b) Jiao, H.; Schleyer, P. v. R. *Angew. Chem., Int. Ed. Engl.* ***1993***, *32*, 1763. (c) Herges, R.; Jiao, H.; Schleyer, P. v. R. *Angew. Chem., Int. Ed. Engl.* **1994**, *33*, 1376.

(28) (a) Schleyer, P. v. R.; Freeman, P.; Jiao, H.; Goldfuss, B. *Angew. Chem., Int. Ed. Engl.* **1995**, *34*, 337. (b) Dauben, H. J., Jr.; Wilson, J. D.; Laity, J. L. *J. Am. Chem. Soc.* **1968**, *90*, 811.

(29) *Gaussian 94*, Revision B.2; Frisch, M. J.; Trucks, G. W.; Schlegel, H. B.; Gill, P. M. W.; Johnson, B. G.; Robb, M. A.; Cheeseman J. R.; Keith, T.; Petersson, G. A.; Montgomery, J. A.; Raghavachari, K.; Al-Laham, M. A.; Zakrzewski, V. G.; Ortiz, J. V.; Foresman, J. B.; Peng, C. Y.; Ayala, P. Y.; Chen, W.; Wong, M. W.; Andres, J. L.; Replogle, E. S.; Gomperts, R.; Martin, R. L.; Fox, D. J.; Binkley, J. S.; Defrees, D. J.; Baker, J.; Stewart, J. S.; Head-Gordon, M.; Gonzalez, C.; Pople, J. A.; Gaussian, Inc.: Pittsburgh, PA, 1995.

(30) (a) Hariharan, P. C.; Pople J. A. *Chem. Phys. Lett.* **1972**, *66*, 217. (b) Hehre, W. J.; Radom, L.; Schleyer, P. v. R.; Pople, J. A. *Ab Initio Molecular Orbital Theory*; Wiley: New York, 1986.

(31) Parr, R. G.; Yang, W. *Density-Functional Theory of Atoms and Molecules*; Oxford: New York, 1989.

(32) (a) Lee, C.; Yang, W.; Parr, R. G. *Phys. Rev. B* **1980**, *37*, 785. (b) Becke, A. D. *Phys. Rev. A* **1988**, *38*, 3098. (c) Becke, A. D. *J. Chem. Phys.* **1993**, *98*, 5648. (d) Kohn, W.; Becke, A. D.; Parr, R. G. *J. Phys. Chem.* **1996**, *100*, 12974 and references therein.

(33) McIver, J. W.; Komornicki, A. K. *J. Am. Chem. Soc.* **1972**, *94*, 2625.

(34) Wolinski, K.; Hilton, J. F.; Pulay, P. *J. Am. Chem. Soc.* **1990**, *112*, 8251.

(35) Fukui, K. *Acc. Chem. Res.* **1981**, *14*, 363. (b) Gonzalez, C.; Schlegel, H. B. *J. Chem. Phys.***1989**, *90*, 2154. (c) Gonzalez, C.; Schlegel, H. B. *J. Phys. Chem.* **1990**, *94*, 5523.

(36) (a) Malkin, V. G.; Malkina, O. L.; Casida, M. E.; Salahub, D. R. *J. Am. Chem. Soc.* **1994**, *116*, 5898. (b) Malkin, V. G.; Malkina, O. L.; Eriksson, L. A.; Salahub, D. R. In *Modern Density Functional Theory*; Seminario, J. M., Politzer, P., Eds.; Elsevier: Amsterdam, 1995; p 273.

(37) (a) St-Amant, A.; Salahub, D. R. *Chem. Phys. Lett.* **1990**, *169*, 387. (b) Godbout, N.; Salahub, D. R.; Andzelm, J.; Wimmer, E. *Can. J. Chem.* **1992**, *70*, 560. (c) Salahub, D. R.; Fournier, R.; Mlynarsky, P.; Papai, I.; St-Amant, A.; Ushio, J. In *Density Functional Methods in Chemistry*; Labanowsky, J., Andzelm, J., Eds.; Springer: New York, 1991; p 77.

(38) Pipek, J.; Mezey, P. G. *J. Chem. Phys.***1989**, *90*, 4916.

(39) Kutzelnigg, W.; Fleischer, U.; Schlinder, M. In *NMR−Basic Principles and Progress*; Springer: Heidelberg, 1990; Vol. 23, p 165.

(40) (a) Perdew, J. P.; Wang, Y. *Phys. Rev. B* **1992**, *45*, 13244. (b) Perdew, J. P.; Chevary, J. A.; Vosko, S. H.; Jackson, K. A.; Pederson, M. R.; Singh, D. J.; Fiolhais, C. *Phys. Rev. B* **1992**, *46*, 6671.

(41) (a) Tomasi, J.; Persico, M. *Chem. Rev.* **1994**, *94*, 2027. (b) Simkin, B. Y.; Sheikhet, I. *Quantum Chemical and Statistical Theory of Solutions−A Computational Approach*; Ellis Horwood: London, 1995; pp. 78−101. (c) Cramer, C. J.; Truhlar, D. G. In *Reviews in Computational Chemistry*; Lipkowitz, K. B., Boyd, D. B., Eds.; VCH Publisher: New York, 1995; Vol. VI, pp 1−72. (d) Morao, I.; Lecea, B.; Arrieta, A.; Cossío, F. P. *J. Am. Chem. Soc.* **1997**, *119*, 826.

(42) Onsager, L. *J. Am. Chem. Soc.* **1936**, *58*, 1486.

(43) (a) Wong, M. W.; Wiberg, K. B.; Frisch, M. J. *J. Am. Chem. Soc.* **1992**, *114*, 523. (b) Wong, M. W.; Wiberg, K. B.; Frisch, M. J. *J. Am. Chem. Soc.* **1992**, *114*, 1645.

(44) (a) Wiberg, K. B.; Castejon, H.; Keith, T. A. *J. Comput. Chem.* **1996**, *17*, 185. (b) Wiberg, K. B.; Keith, T. A.; Frisch, M. J.; Murcko, M. *J. Phys. Chem.* **1995**, *99*, 9072. (c) Wiberg, K. B.; Rablen, P. R.; Rush, D. J.; Keith, T. A. *J. Am. Chem. Soc.* **1995**, *117*, 4261.

(45) Reichardt, C. *Solvents and Solvent Effects in Organic Chemistry*; VCH: Weinheim, 1990.

(46) (a) Dewar, M. J. S. *J. Am. Chem. Soc.* **1984**, *106*, 209. (b) Borden W. T.; Loncharich, R. J.; Houk K. N. *Annu. Rev. Phys. Chem.* **1988**, *39*, 213.

(47) Leroy has proposed the term "asynchronism" in similar contexts. See: Leroy, G.; Sana, M. *Tetrahedron* **1975**, *31*, 2091.

(48) Moyano, A.; Pericàs, M. A.; Valentí, E. *J. Org. Chem.* **1989**, *54*, 573.

(49) (a) Lecea, B.; Arrieta, A.; Roa, G.; Ugalde, J. M.; Cossío, F. P. *J. Am. Chem. Soc.* **1994**, *116*, 12314. (b) Lecea, B.; Arrieta, A.; Lopez, X.; Ugalde, J. M.; Cossío, F. P. *J. Am. Chem. Soc.* **1995**, *117*, 12314.

Table 1. Activation Energies[a] (ΔE_a, kcal/mol) and Energies of Reaction[a] (ΔE_{rxn}, kcal/mol) Calculated for the Reactions between Dipoles **1a,b** and Dipolarophiles **2a,b**

	$\epsilon = 1.00$		$\epsilon = 35.94$ (L1A1)		$\epsilon = 35.94$ (SCIPCM)	
reaction	ΔE_a	ΔE_{rxn}	ΔE_a	ΔE_{rxn}	ΔE_a	ΔE_{rxn}
1a + **2a** → **3aa**	15.05	−75.16	17.02	−73.52	16.07	−72.69
1a + **2b** → **3ab**	14.60	−37.07	16.74	−36.58	15.93	−36.88
1b + **2a** → **3ba**	19.87	−42.14	17.84	−39.60	19.31	−36.63
1b + **2b** → **3bb**	16.57	−23.90	18.64	−21.05	19.31[b]	−19.63[b]

[a] Relative energies at the B3LYP/6-31+G*+ΔZPVE level. [b] Single-point energy computed at the B3LYP(SCIPCM)/6-31+G*//B3LYP-(L1A1)/6-31+G*+ΔZPVE level (see text).

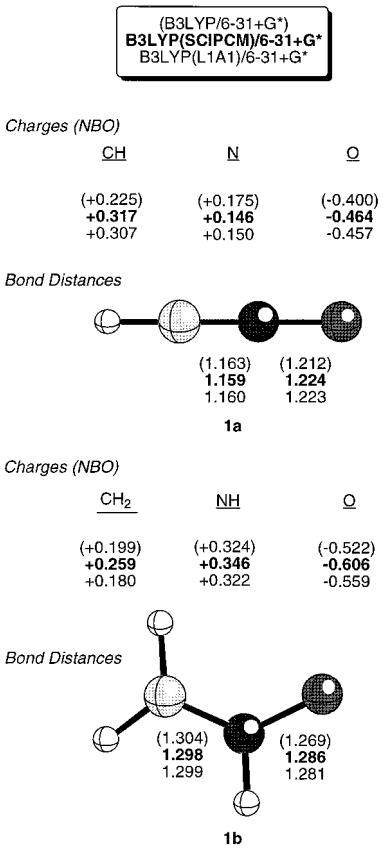

Figure 1. Bond distances (Å) and NBO charges of dipoles **1a** (fulminic acid) and **1b** (nitrone) computed at different theoretical levels. The L1A1 and SCIPCM data have been computed with $\epsilon = 35.94$ (acetonitrile). In this and the following figures which incorporate ball-and-stick representations, atoms are represented by increasing order of shadowing as follows: H, C, O, N.

$$\delta B_i = \frac{B_i^{TS} - B_i^{R}}{B_i^{P} - B_i^{R}} \quad (2)$$

The superscripts R and P refer to the reactant and the product, respectively. The average value of δB_i, denoted as δB_{av} in eq 1, therefore is

$$\delta B_{av} = n^{-1}\sum_{i=1}^{n} \delta B_i \quad (3)$$

Wiberg indices[50] B_i were employed; these were evaluated by using the natural bond orbital (NBO)[51,52] method.

(50) Wiberg, K. B. *Tetrahedron* **1968**, *24*, 1083.

(51) (a) Reed, A. E.; Weinstock, R. B.; Weinhold, F. *J. Chem. Phys.* **1985**, *83*, 735. (b) Reed, A. E.; Curtiss, L. A.; Weinhold, F. J. *Chem. Rev.* **1988**, *88*, 899.

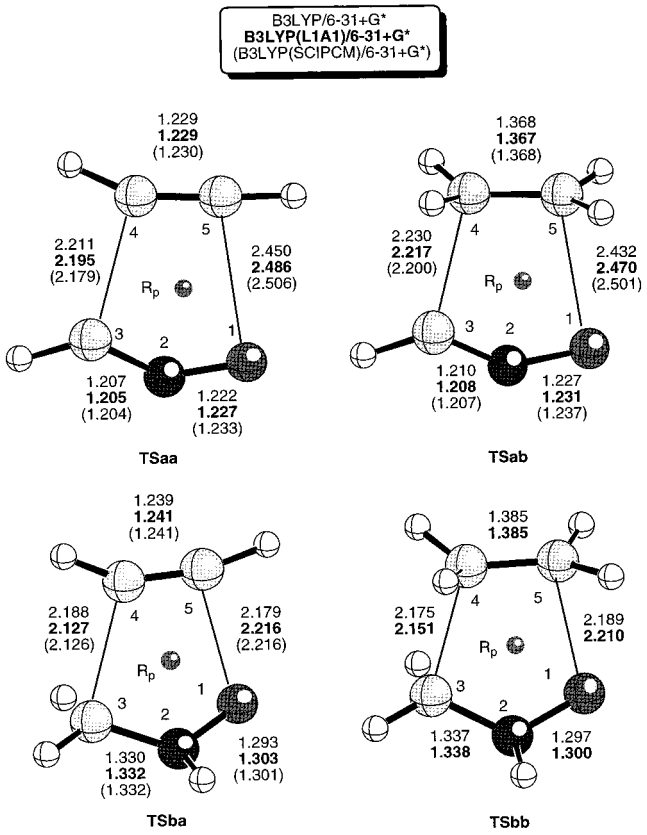

Figure 2. Bond distances (Å) of transition structures **TSaa**−**bb** computed at different theoretical levels. R_p denotes the ring point of electron density. The L1A1 and SCIPCM data have been obtained with $\epsilon = 35.94$ (acetonitrile). It was not possible to optimize the **TSbb** structure at the B3LYP(SCIPCM)/6-31+G* level because of convergence problems. On the basis of the remaining L1A1 and SCIPCM data, the L1A1geometry obtained for **TSbb** should be accurate enough.

Results and Discussion

We first studied the reactions of the simplest N,O-dipolarophiles, fulminic acid (**1a**) and nitrone (**1b**), with ethylene and with acetylene (see Scheme 1). The activation and reaction energies in the gas phase (taken from our previous paper[21]) are compared with those in acetonitrile solution in Table 1. The main geometric parameters of **1a**, **1b**, the transition structures, and products are shown in Figures 1 and 2 and in Figure S1 of the Supporting Information.

The structural data in Figure 1 demonstrate that the solvent polarizes the dipoles **1a,b** yielding structures with 0.01−0.02 Å larger N−O bond distances, slightly shorter C−N distances, and larger N(+)−O(−) NBO charge differences. It is noteworthy that the computationally much lesser demanding L1A1 level yields geometries which do not differ significantly from those obtained at the more sophisticated SCIPCM level, despite the nonspherical character of the dipoles **1a,b**.

Similar conclusions can be drawn from analysis of the structural parameters of the four saddle points in Figure 2. The solvent increases the O1−C5 but shortens the C3−C4 distances. Once again, the L1A1 and the SCIPCM results are quite similar, particularly for **TSba**.

The data included in Table 1 indicate that the energies of activation of these processes are larger in solution than in the gas phase, whereas the reaction energies are lower. This can be explained by the higher solvation energies of the 1,3-dipoles.

(52) NBO: Glendening, E. D.; Reed, A. E.; Carpenter, J. E.; Weinhold, F., NBO Version 3.1, 1995; Gaussian, Inc.

Table 2. Synchronicities[a] (Sy) and Nucleus-Independent Chemical Shifts[b] (NICS, ppm mol^{-1}) of the Reactions between Dipoles **1a,b** and Dipolarophiles **2a,b**

	$\epsilon = 1.00$			$\epsilon = 35.94$		
reaction	NICS (**TS**)	NICS (**3**)	Sy	NICS (**TS**)	NICS (**3**)	Sy
1a + **2a** → **3aa**	−17.82	−12.30	0.80	−17.14	−12.22	0.71
1a + **2b** → **3ab**	−20.08	−5.15	0.79	−19.33	−5.21	0.72
1b + **2a** → **3ba**	−17.83	−7.25	0.92	−17.85	−7.26	0.87
1b + **2b** → **3bb**	−21.20	−9.24	0.92	−21.12	−9.27	0.87

[a] Computed at the B3LYP/6-31+G* and B3LYP(L1A1)/6-31+G* levels with eqs 1−3 (see text). [b] Computed at the GIAO−SCF/6-31+G*//B3LYP/6-31+G* and GIAO-SCF/6-31+G*//B3LYP(L1A1)/6-31+G* levels.

The large zwitterionic character of the 1,3-dipoles diminishes along the reaction coordinate, thereby resulting in lower solvation energies for the transition structures and the reaction products. A similar effect has been observed experimentally in [3+2] cycloaddition between nitrones and alkenes.[19,53] Figure S2 of the Supporting Information shows the linear correlation between the activation energies, computed at the B3LYP-(SCIPCM) level for the **1b** + **2b** → **3bb** reaction in several solvents and the Onsager function, $(\epsilon - 1)/(2\epsilon + 1)$.

The computed synchronicities of the reactions between dipoles **1a,b** and dipolarophiles **2a,b** (Scheme 1) are lower in solution ($\epsilon = 35.95$) than in the gas phase (Table 2). Moreover, the computed synchronicities of the **1b** + **2b** → **3bb** reaction in different solvents show a linear correlation with the activation energy (Figure S3 of the Supporting Information). Therefore, this type of reaction is more asynchronous and has higher activation energies in more polar solvents. This contrasts with other [2+2][54] and [4+2][55] cycloadditions in which the transition structures are more polar than the reactants, thereby resulting in lower activation energies in solvents.

We have also investigated the aromaticity of both the transition structures and the reaction products of the reactions between **1a,b** and **2a,b**. In Table 2 we report the NICS for the transition structures **TSaa**−**TSbb** and cycloadducts **3aa**−**3bb**. These positions chosen are the (3,+1) ring points of electron density as defined by Bader,[56] which constitutes an unambiguous characterization of a ring.[21,56] The large negative NICS values exhibited by all four saddle points, both in the gas phase and in solution, indicate the strong aromatic character. In contrast, with the exception of π-aromatic isoxazole **3aa**, the remaining cycloadducts show lower NICS values, motivated by diamagnetic shielding induced by the lone pairs. While the NICS values computed in solution are lower than those obtained in the gas phase, the differences are very small. Therefore, aromaticity does not appear to be very sensitive to solvent effects in these compounds.[57] IRC calculations in the gas phase and in simulated acetonitrile solution agree with this conclusion. Figure 3 shows the NICS values plotted against the IRC for the **1a** + **2a** → **3aa** reaction. The NICS values at the center of masses for the reactants, transition structure and products in the gas phase and in solution coincide. However, the decrease in aromaticity from **TSaa** to **3aa** is more pronounced in acetonitrile solution than in the gas phase (Figure 3). In this case *in-plane* aromaticity "quenches" more rapidly in solution than in vacuo and NICS reaches the value associated with the π-aromatic isoxazole **3aa** more rapidly. In contrast, the NICS vs IRC profile of the **1b** + **2b** → **3bb** process in which a nonaromatic cycloadduct is formed shows an almost complete coincidence between the gas

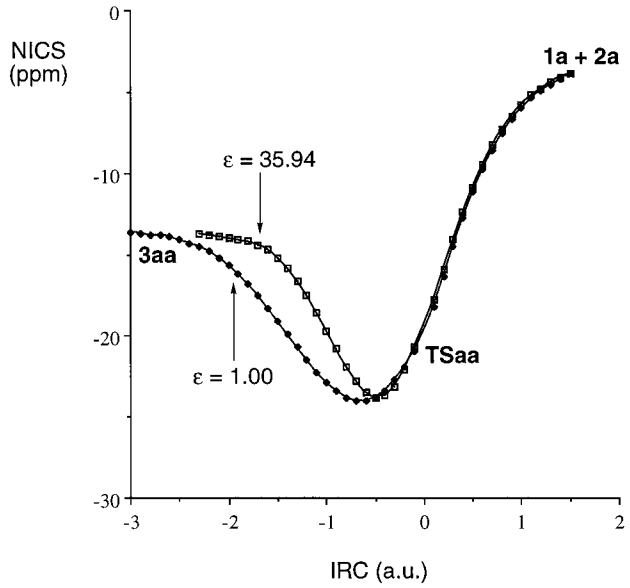

Figure 3. NICS vs IRC profiles for the reaction between fulminic acid (**1a**) and acetylene (**2a**) to yield isoxazole (**3aa**) in the gas phase ($\epsilon = 1.00$) and in solution ($\epsilon = 35.94$). The NICS values have been computed at the center of masses of the whole system, since for points earlier than **TSaa** the (3,+1) ring point is not defined. The NICS values have been computed at the SOS-DFPT-IGLO/IGLO-III TZ2P level on either B3LYP/6-31+G* or B3LYP(SCIPCM)/6-31+G* geometries.

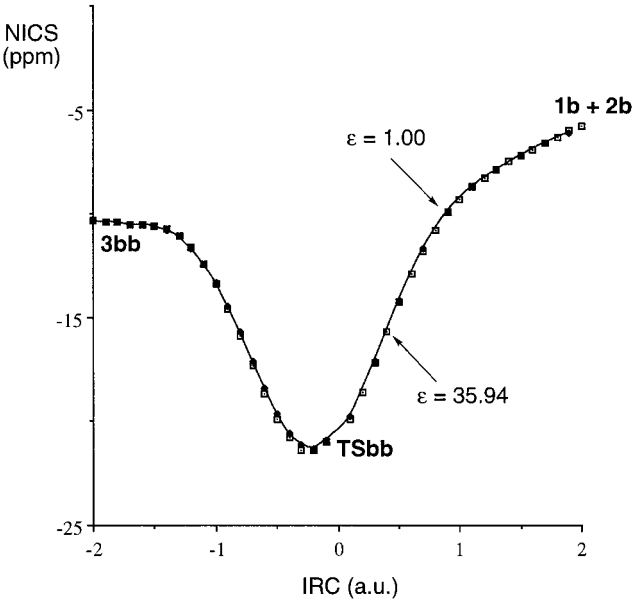

Figure 4. NICS vs IRC profiles for the reaction between nitrone (**1b**) and acetylene (**2b**) to yield isoxazolidine (**3bb**) in the gas phase ($\epsilon = 1.00$) and in solution ($\epsilon = 35.94$). See Figure 3 caption for additional details.

(53) (a) Huisgen, R.; Seidl, H.; Brüning, I. *Chem. Ber.* **1969**, *102*, 1102. (b) Kadaba, P. K. *Synthesis* **1973**, 71.

(54) (a) Huisgen, R.; Feier, L. A.; Otto, P. *Tetrahedron Lett.* **1968**, 4485. (b) Huisgen, R. *Angew. Chem., Int. Ed. Engl.* **1969**, *7*, 348. (c) Huisgen, R. *Acc. Chem. Res.* **1977**, *10*, 117. (d) Lim, D.; Jorgensen W. L. *J. Phys. Chem.* **1996**, *100*, 17490.

(55) (a) Berson, J. A.; Hamlet, Z.; Mueller, W. A. *J. Am. Chem. Soc.* **1962**, *84*, 297. (b) Grieco, P. A.; Garner, P.; He, Z. *Tetrahedron Lett.* **1983**, *24*, 1897. (c) Jorgensen, W. L.; Blake, J. F.; Dongchul, L.; Severance, D. L. *J. Chem. Soc., Faraday Trans.* **1994**, *90*, 1727. (d) Sustmann, R.; Sicking, W. *J. Am. Chem. Soc.* **1996**, *118*, 12562.

(56) Bader, R. F. W. *Atoms in Molecules*−*A Quantum Theory*; Clarendon Press: Oxford, 1990; pp 13−52.

(57) Katritzky et al. have reported aromaticity variations with molecular environment for several polar aromatic hydrocarbons such as azulene and nitrogen-containing heterocycles. See: Katritzky, A. R.; Karelson, M.; Wells, A. P. *J. Org. Chem.* **1996**, *61*, 1619.

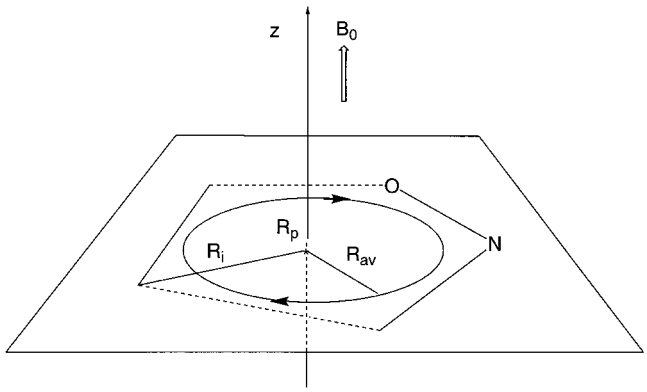

Figure 5. Schematic definition of an in-plane ring current for **TSaa** as well as the variables included in eqs 4 and 5. R_p stands for the (3,+1) ring point of electron density.

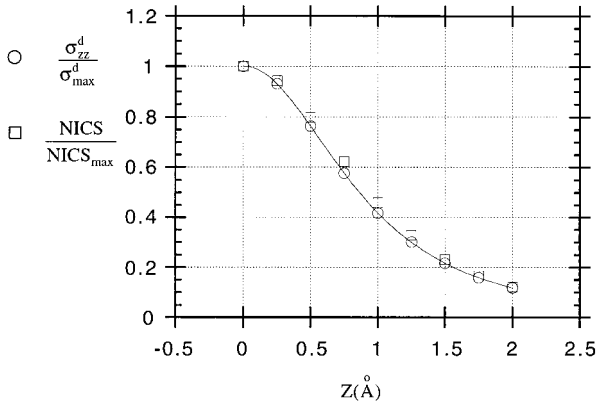

Figure 6. NICS/NICSmax and $\sigma^d_{zz}/\sigma^d_{max}$values for **TSaa** plotted against the *z*-axis as defined in Figure 5. The NICS values have been computed at the GIAO-SCF/6-31+G*//B3LYP/6-31+G* level. The $\sigma^d_{zz}/\sigma^d_{max}$values have been computed by using eqs 4−6.

phase and solution profiles. In addition, note that the maximum NICS values are reached beyond the transition structures (IRC = 0) in both Figures 3 and 4. This feature will be examined later.

In our communication,[21] we reported that the variation of the NICS values along the axis perpendicular to the molecular plane and which intersects the (3,+1) critical ring point permits the characterization of both *in-plane* and π-aromaticity. This behavior is compatible with the ring-current model.[58] In a previous paper,[59] we have shown that for an in-plane ring current moving in the molecular plane, the variation of the diamagnetic shielding σ^d_{zz} along the *z*-axis perpendicular to such a plane (Figure 5) is given by eq 4:

$$\sigma^{d}_{zz} = -\frac{e^2\mu_o}{8\pi m_e}R_{av}^{-1}\left[1+\left(\frac{z}{R_{av}}\right)^2\right]^{-3/2} \quad (4)$$

Here, R_{av}, the average radius with respect to the (3,+1) ring point, is defined as

$$R_{av} = n^{-1}\sum_{i=1}^{n}\left(R_i - \frac{4}{Z_i}a_o\right) \quad (5)$$

where R_i is the distance of the *i*th-nucleus to the ring point, Z_i is the atomic number of the *i*th-nucleus, and a_o is the Bohr radius. The $(4/Z_i)a_o$ term of eq 5 corresponds to the maximum of the radial probability function $4\pi r^2R^2_{n,l}(r)$ for a 2p atomic orbital.

According to eq 4, the maximum diamagnetic shielding σ^d_{max} for an *in-plane* aromatic transition structure occurs when $z = 0$ and therefore

$$\sigma^{d}_{max} = -\frac{e^2\mu_0}{8\pi m_e}R_{av}^{-1} \quad (6)$$

On the basis of eq 5 and the geometric data reported in Figure 2, we have obtained $R_{av} = 1.127$ Å for **TSaa**, in the gas phase. Equation 6 (i.e., eq 4 with $z = 0$), gives $\sigma^d_{max} = -12.5$ ppm. This value compares well with the maximum NICS obtained at the GIAO-SCF/6-31+G*//B3LYP/6-31+G* level ($NICS_{max} = -17.8$ ppm, Table 2). The diamagnetic shielding in aromatic structures is known to be due in part to local effects.[60] Hence, we can conclude that the ring current model accounts for ca. 70% of the total diamagnetic shielding. We also have calculated the variation of this ratio along the *z*-axis by means of eq 4. The results, displayed in Figure 6, demonstrate that eq 4 describes correctly the variation of the diamagnetic effect of the ring current above and below the molecular plane:

$$\frac{\sigma^{d}_{zz}}{\sigma^{d}_{max}} \approx \frac{NICS}{NICS_{max}} \quad (7)$$

In summary, the diamagnetic effect of an *in-plane* ring current associated with an aromatic transition structure decays monotonically along the *z*-axis from the molecular plane.

Equations 4−6 also provide a basis for understanding the behavior of the NICS along the reaction paths shown in Figures 3 and 4: after the transition structure (going from right to left), the R_{av} parameter decreases and the diamagnetic shielding induced by the electronic circulation increases, thus increasing the NICS. However, after a certain point on the reaction coordinate, formation of the new σ bonds is more advanced. This counteracts the cyclic electron delocalization, thereby decreasing the diamagnetic shielding at the center of the ring. In contrast, the contraction of the ring radius during the **1a** + **2a** → **3aa** reaction increases π-aromaticity, since this requires parallel overlap among the p-AO's. Therefore, the difference between the NICS at the TS and the maximun NICS along the IRC in Figure 3 is larger than in Figure 4.

The π-aromatic compound oxazole (**3aa**), can be considered to have two ring currents circulating at a distance R_0 above and below the molecular plane (Figure 7).[61] On this basis, a treatment similar to that used in developing eq 4[59] gives the following expression for the diamagnetic shielding along the *z*-axis:

$$\sigma^{d}_{zz} = -\frac{e^2\mu_0}{16\pi m_e}R_{av}^{-1}\left\{\left[1+\left(\frac{z-R_0}{R_{av}}\right)^2\right]^{-3/2} + \left[1+\left(\frac{z+R_0}{R_{av}}\right)^2\right]^{-3/2}\right\} \quad (8)$$

In this expression, R_{av} is the average radius from the ring critical

(58) (a) Pauling, L. *J. Chem. Phys.* **1936**, *4*, 673. (b) London, F. *J. Phys. Radium* **1937**, *8*, 397. (c) Pople, J. A. *J. Chem. Phys.* **1956**, *24*, 1111. (d) Schneider, W. G.; Bernstein, H. J.; Pople, J. A. *J. Am. Chem. Soc.* **1958**, *80*, 3497. (e) Haig, C. W.; Maillon, R. B. *Prog. Nucl. Magn. Reson. Spectrosc.* **1980**, *13*, 303.

(59) Morao, I.; Cossío, F. P. *J. Org. Chem.* **1999**, *64*, 1868.

(60) (a) Fleischer, U.; Kutzelnigg, W.; Lazzaretti, P.; Muhllenkamp, V. *J. Am. Chem. Soc.* **1974**, *116*, 5298. (b) Fowler, P. W.; Steiner, E. *J. Phys. Chem.* **1997**, *101*, 1409. (c) Schleyer, P. v. R.; Jiao, H.; Hommes, N. J. R. v. E.; Malkin, V.; Malkina, O. L. *J. Am. Chem. Soc.* **1997**, *119*, 12669.

(61) Farnum, D. G.; Wilcox, C. F. *J. Am. Chem. Soc.* **1967**, *89*, 5379.

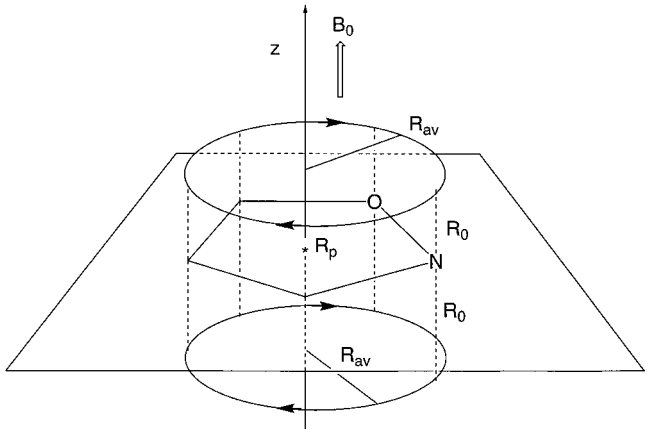

Figure 7. Schematic definition of two π-ring currents for isoxazole (**3aa**) as well as the variables included in eqs 8−10. R_p stands for the (3,+1) ring point of electron density.

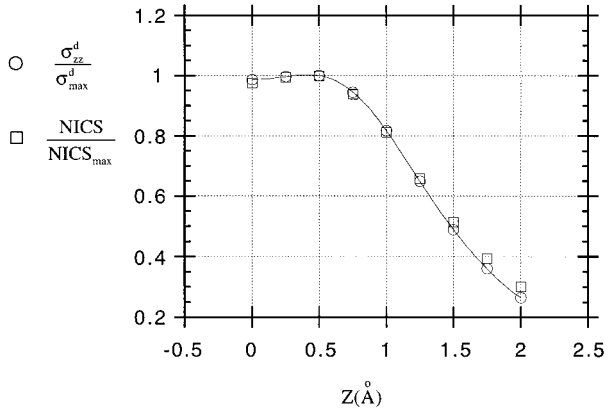

Figure 8. NICS/$NICS_{max}$ and $\sigma_{zz}^d/\sigma_{max}^d$ values for **3aa** plotted against the *z*-axis as defined in Figure 7. The NICS values have been computed at the GIAO-SCF/6-31+G*//B3LYP/6-31+G* level. The $\sigma_{zz}^d/\sigma_{max}^d$values have been computed by using eqs 8−10.

point to the five nuclei of the aromatic ring:

$$R_{av} = n^{-1}\sum_{i=1}^{n} R_i \qquad (9)$$

R_0 is estimated from Pauling's[62] covalent radii r_i^{cov} of the five heavy atoms of isoxazole

$$R_0 = n^{-1}\sum_{i=1}^{n} r_i^{cov} \qquad (10)$$

Equations 9 and 10, with the geometry of isoxazole in Figure S1 of the Supporting Information, give R_{av} = 1.164 Å and R_0 = 0.67 Å for **3aa**. A numerical interpolation of σ_{zz}^d values at different values of *z* yields a maximum value of $\sigma_{max}^d = -8.0$ ppm for z = 0.43 Å. Similarly, at z = 0.5 Å, the GIAO-SCF/6-31+G*//B3LYP/6-31+G* computation gives $NICS_{max}$ = −12.6 ppm.

A plot of the $\sigma_{zz}^d/\sigma_{max}^d$ ratio at different *z* values, shown in Figure 8, is found to agree well with the NICS/$NICS_{max}$ vs *z* curve. Therefore, eq 7 also holds for π-aromatic structures. Hence, the ring current model as expressed by eqs 4 and 8 can be used to characterize both *in-plane* and π-aromaticity. The diamagnetic-based shielding does not decay monotonically as in the case of *in-plane* aromaticity. Instead, the σ_{zz}^d or $NICS_z$ maximum value is not found in the molecular plane, but at a distance from this plane, which is closely related to the covalent radii of the atoms of the ring.

Scheme 4

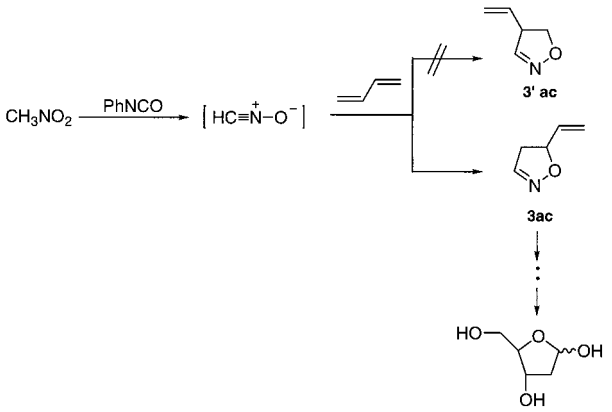

Regiochemistry. The regiochemistry of these reactions has been investigated employing the reaction between fulminic acid (**1a)** and 1,3-butadiene (**2c**). This reaction was used by Torssell et al. to prepare D,L-deoxysugars.[63] When fulminic acid was generated in situ from nitromethane, only the 5-substituted isoxazoline **3ac** was obtained (Scheme 4). We have calculated the transition structures **TS′ac** and **TSac**, associated with the formation of the isomeric isoxazolines **3′ac** and **3ac**, respectively (Figure 9). The corresponding activation energies as well as reaction energies are reported in Table 3. The reaction energy of the **1a** + **2c** → **3ac** process is ca. 4.6 kcal/mol lower than that calculated for the parent reaction **1a** + **2b** → **3ab** in the gas phase (see Tables 1 and 3). The conjugation energy of 1,3-butadiene, estimated by means of the related eq 11, is ΔE= +4.5 kcal/mol.[64]

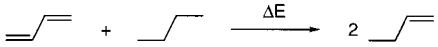

(11)

Therefore, we can conclude that the lower energy of reaction calculated for the **1a** + **2c** → **3ac** process can be explained entirely in terms of the loss of conjugation in the substrate. In contrast, the activation energy for this reaction is almost identical with that calculated for the parent reaction in the gas phase. The transition structure associated with the formation of **3′ac** is found to be 3.32 kcal/mol higher in energy than **TSac** in the gas phase. Therefore, the B3LYP/6-31+G* calculations favor formation of **3ac** strongly, in good agreement with the experimental evidence. Note that **TSac** is slightly more polar, less synchronous, and less aromatic than **TS′ac**. *Aromaticity is important but it does not determine the regioselectivity of the reaction*. The same conclusion is reached from results in chloroform solution (ϵ = 4.81, see Table 3). Thus, despite its lower NICS value, **TSac** is found to be 3.46 kcal/mol lower in energy than **TS′ac** at the B3LYP(L1A1)/6-31+G*, a value very close to that calculated in the gas phase. Therefore, in this reaction the regioselectivity is controlled by the more favorable energy of the product rather than by the relative aromaticities of the regioisomeric transition structures. We have calculated the energy density H(**r**) at the (3,−1) bond critical point between

(62) Pauling, L. *The Nature of the Chemical Bond*, 3rd ed.; Cornell University Press: Ithaca, 1960; p 224.

(63) Torssell, K. B. G.; Hazell, A. C.; Hazell, R. G. *Tetrahedron* **1985**, *41*, 5569.

(64) The total energies (au) at the B3LYP/6-31+G*+ZPVE level of compounds included in eq 11 are the following: 1,3-butadiene, −155.91588; *n*-butane, −158.33084; 1-butene, −157.11982.

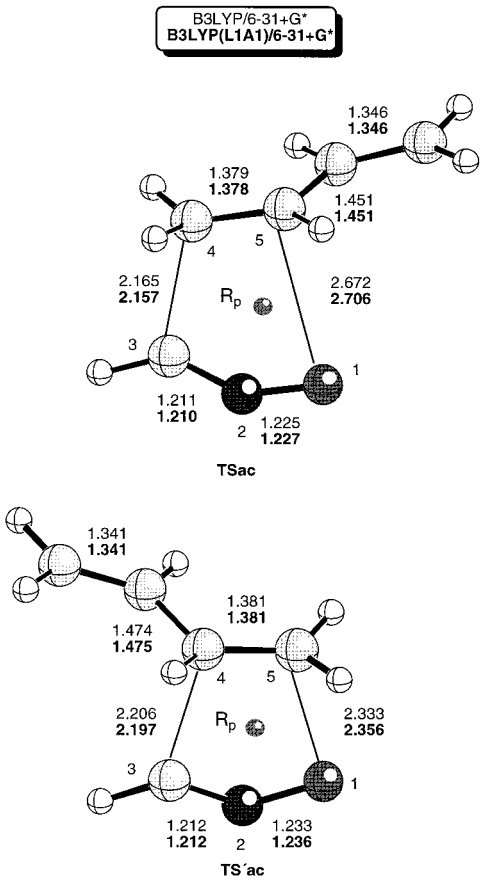

Figure 9. Bond distances (Å) of transition structures **TSac** and **TS′ac** computed at different theoretical levels. R_p denotes the ring point of electron density. The L1A1 data have been obtained with $\epsilon = 4.81$ (chloroform).

Table 3. Calculated Activation Energies[a] (ΔE_a, kcal/mol), Energies of Reaction[a] (ΔE_{rxn}, kcal/mol), Synchronicities[b,c] (Sy), NICS[d] (ppm mol^{-1}), and Dipole Moments[b] of the Transition Structures (μ_{TS}, au) for the Reaction between Fulminic Acid (**1a**) and 1,3-Butadiene (**2c**)

	1a + **2c** → **3ac**		**1a** + **2c** → **3′ac**	
magnitude	$\epsilon = 1.00$	$\epsilon = 4.81$	$\epsilon = 1.00$	$\epsilon = 4.81$
ΔE_a	14.61	16.15	17.93	19.61
ΔE_{rxn}	−32.45	−31.68	−30.24	−29.34
Sy	0.71	0.66	0.84	0.81
NICS	−14.41	−13.78	−20.89	−20.48
μ_{TS}	1.11	1.33	0.97	1.22

[a] Values computed at the B3LYP/6-31+G*+ΔZPVE and B3LYP-(L1A1)/6-31+G*+ΔZPVE levels for $\epsilon = 1.00$ and 4.81, respectively. [b] Values computed at the B3LYP/6-31+G* and B3LYP(L1A1)/6-31+G* levels for $\epsilon = 1.00$ and 4.81, respectively. [c] Computed with eqs 1−3 (see text). [d] Computed at the GIAO-SCF/6-31+G*//B3LYP/6-31+G* and GIAO-SCF/6-31+G*//B3LYP(L1A1)/6-31+G* levels for $\epsilon = 1.00$ and 4.81, respectively.

O1 and C5[65] using the expression

$$H(\mathbf{r}) = {}^1/_4\nabla^2\rho(\mathbf{r}) - G(\mathbf{r}) \qquad (12)$$

where $G(\mathbf{r})$ and $\rho(\mathbf{r})$ are the kinetic energy density and the electron density, respectively. For **TS′ac**, the $H(\mathbf{r})$ value between O1 and C5 is −1.13 kcal/Å^3, which indicates that the O1−C5 bond being formed is covalent. In contrast, the same value for **TSac** is found to be +3.14 kcal/Å^3, which corresponds to an ionic interaction.[66] Therefore, our calculations indicate that in the more polar saddle point **TSac** the interaction between the O1 atom and the allyl moiety is mainly electrostatic in nature. The large O1−C5 bond distance results in poor overlap, and covalency, between both atoms, thereby making it difficult to determine the diamagnetic ring current associated with aromaticity. Therefore, in this particular case the most polar transition structure (**TSac**) is the less synchronous and the less aromatic (than **TS′ac**) structure.

Scheme 5

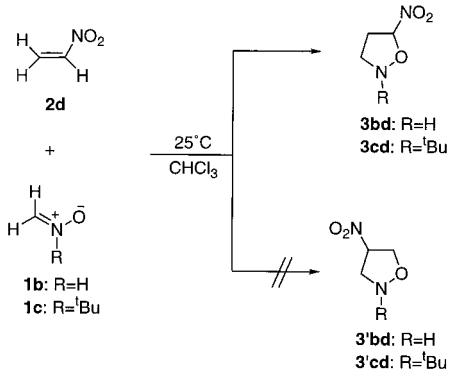

We also have investigated the reactivity of nitrone (**1b**) toward a π-deficient dipolarophile, nitroethylene (**2d**). An analogous transformation was studied by Houk et al. experimentally[67] (Scheme 5). These authors observed exclusive formation of the 5-substituted cycloadduct **3cd** in chloroform at 25 °C, instead of the 4-substituted regioisomer **3′cd**, which is preferred when C-substituted nitrones are used.[67,68] In the reaction of nitrones with substituted alkenes, aside from the regioisomeric transition structures and products, there are two possible endo and exo stereoisomers, depending upon the relative orientation of the substituent of the nitroalkene and the central atom of the allyl anion-type dipole. For example, the *supra-supra* approach between the reactants gives rise to two possible stereoisomeric 5-substituted transition structures:

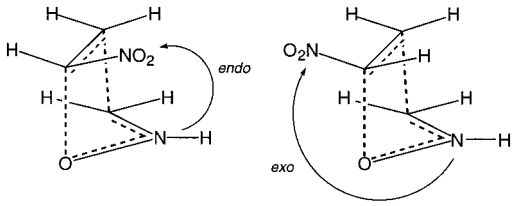

Similarly, the 5-substituted cycloadducts can adopt either endo *or* exo conformations.

We have located four transition structures for the reaction between nitrone and nitroethylene on the B3LYP/6-31+G* energy hypersurface, both in isolation (gas phase) and in simulated chloroform solution. The chief geometric features of these transition structures and cycloadducts are displayed in Figures 10 and S4 of the Supporting Information, respectively. Relevant data for this reaction are reported in Table 4. According to our results the endo transition structures are ca. 3 kcal/mol more stable than the exo TS's. This preference is not retained in the cycloadducts (see Table 4). Our B3LYP/6-31+G* calculations favor preferential formation of the 4-substituted cycloadduct **3′bd**, a result that is *not* in agreement with the

(65) Cremer, D.; Kraka, E. *Croat. Chem. Acta* **1989**, *57*, 1259.

(66) For other applications of the $H(\mathbf{r})$ criterion in the determination of the ionic or covalent character of bonds, see: (a) Lecea, B.; Arrieta, A.; Morao, I.; Cossío, F. P. *Chem. Eur. J.* **1997**, *3*, 20. (b) Lopez, X.; Ugalde, J. M.; Cossío, F. P. *J. Am. Chem. Soc.* **1996**, *118*, 2718.

(67) Sims, J.; Houk, K. N. *J. Am. Chem. Soc.* **1973**, *95*, 5798−5800.

(68) Houk, K. N.; Bimanand, A.; Mukherjee, D.; Sims, J.; Chang, Y.-M.; Kaufman, D. C.; Domelsmith, L. N. *Heterocycles* **1977**, *7*, 293.

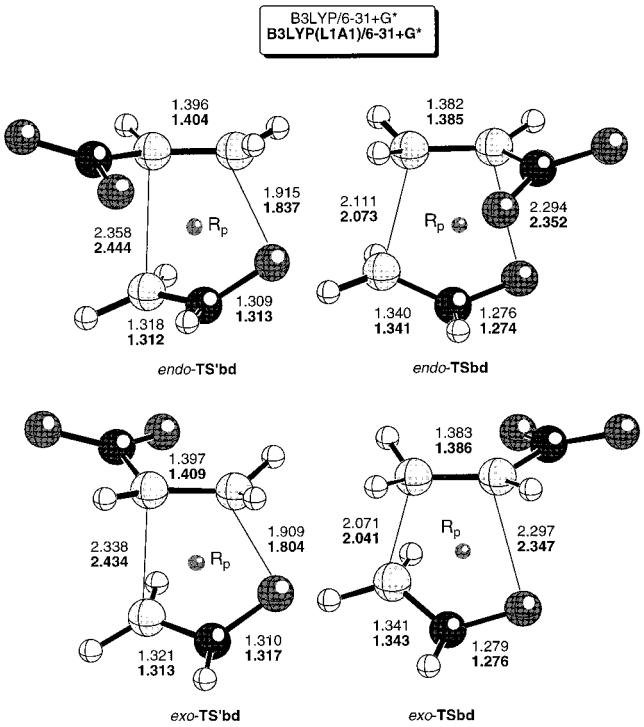

Figure 10. Bond distances (Å) of the four possible transition structures associated with the (3+2) interaction between nitrone and nitroethylene. R_p denotes the ring point of electron density. The L1A1 data have been obtained with $\epsilon = 4.81$ (chloroform).

Table 4. Calculated Activation Energies[a] (ΔE_a, kcal/mol), Relative Activation Energies[a,b] ($\Delta\Delta E_a$, kcal/mol), Energies of Reaction[a] (ΔE_{rxn}, kcal/mol), Synchronicities[c,d] (Sy), NICS[e] (ppm mol^{-1}), and Dipole Moments[c] of the Transition Structures (μ_{TS}, au) for the Reaction between Nitrone (**1b**) and Nitroethylene (2**d**)

	1b + 2d → 3bd		**1b + 2d → 3′bd**	
magnitude	*endo*-**TSbd**	*exo*-**TSbd**	*endo*-**TS′bd**	*exo*-**TS′bd**
		$\epsilon = 1.00$		
ΔE_a	8.84	11.61	8.55	11.62
$\Delta\Delta E_a$	0.00	+2.76	−0.30	+2.77
ΔE_{rxn}	−26.83	−24.33	−23.18	−21.14
Sy	0.70	0.74	0.82	0.84
NICS	−22.36	−21.03	−19.49	−18.27
μ_{TS}	2.44	2.98	1.46	2.29
		$\epsilon = 4.81$		
ΔE_a	8.84	11.81	11.62	12.90
$\Delta\Delta E_a$	0.00	+2.96	+2.77	+4.05
ΔE_{rxn}	−23.49	−22.09	−16.09	−17.78
Sy	0.61	0.64	0.77	0.77
NICS	−21.69	−20.59	−18.08	−16.50
μ_{TS}	3.26	3.57	2.05	3.08

[a] Values computed at the B3LYP/6-31+G*+ΔZPVE and B3LYP-(L1A1)/6-31+G*+ΔZPVE levels for $\epsilon = 1.00$ and 4.81, respectively. [b] Computed with respect to *endo*-**TSbd**. [c] Values computed at the B3LYP/6-31+G* and B3LYP(L1A1)/6-31+G* levels for $\epsilon = 1.00$ and 4.81, respectively. [d] Computed with eqs 1−3 (see text). [e] Computed at the GIAO-SCF/6-31+G*//B3LYP/6-31+G* and GIAO-SCF/6-31+G*//B3LYP(L1A1)/6-31+G* levels for $\epsilon = 1.00$ and 4.81, respectively.

experimental finding (vide supra). However, almost exclusive formation of 5-nitroisoxazoline (**3bd**) via *endo*-**TSbd** is predicted at the B3LYP(L1A1)/6-31+G* level in chloroform solution. In this case, the lowest energy saddle point is the most aromatic and the most asynchronous in solution (see Table 4). In addition, the dipole moments indicate that the transition structures associated with the formation of the 5-nitro cycloadduct are significantly more polar than their corresponding 4-nitro regioisomers. Therefore, if we assume that the electrostatic contribution of the solvation energy can be expressed in terms of the Onsager model and that the cavitation and dispersion energies of *endo*-**TSbd** and *endo*-**TS′bd** are similar in magnitude,[69] their solvation energies, ΔG_{TS} and $\Delta G_{TS'}$, satisfy the following ratio:

$$\frac{\Delta G_{TS}}{\Delta G_{TS'}} \approx \frac{\mu_{TS}^2 a_{TS'}^3}{\mu_{TS'}^2 a_{TS}^3} \tag{13}$$

where ΔG_{TS} and $\Delta G_{TS'}$ are the solvation energies of *endo*-**TSbd** and *endo*-**TS′bd**, respectively, and μ and a are the corresponding dipole moments and cavity radii. The difference in energy of activation in solution can be approximated as

$$\Delta\Delta E_a^{(s)} = \Delta E_{TS}^{(s)} - \Delta E_{TS'}^{(s)} \approx \Delta\Delta E_a^{(g)} - \left(\frac{\epsilon - 1}{2\epsilon + 1}\right)\frac{\mu_{TS'}^2}{a_{TS'}^3}\left[\frac{\mu_{TS}^2 a_{TS'}^3}{\mu_{TS'}^2 a_{TS}^3} - 1\right] \tag{14}$$

where $\Delta\Delta E_a^{(g)}$ is the difference in activation energies in the gas phase. Using eq 14 and the data reported in Table 4 for *endo*-**TSbd** and *endo*-**TS′bd**, we obtain $\Delta\Delta E_a^{(s)} = +1.31$ kcal/mol if the gas-phase dipole moments are used. In contrast, the dipole moments computed in solution lead to $\Delta\Delta E_a^{(s)} = -3.1$ kcal/mol, in good agreement with the relative value obtained at the B3LYP/6-31+G*+ΔZPVE level (Table 4). Hence, solvent effects govern the regiochemistry of this reaction. The polarization of the solute must be taken into account to describe the different reaction paths correctly.

In summary, our study indicates that the regiochemistry of these reactions cannot be assigned by using simple electronic arguments. Since the aromaticity indices reflect intramolecular stereoelectronic effects, our results are useful to assign the impact of steric and polar (including solvent) effects to the regio- and stereochemical outcome. It is noteworthy that previous studies have detected the importance of nonstereoelectronic effects in these kinds of reactions.[70] On the other hand, previous studies have also shown that FMO theory can fail in several cases to describe the regio- and stereoselectivity of 1,3-dipolar reactions.[69,71] Similar disagreement can be found when the HSAB theory is applied to this reaction.[72]

Conclusions

From the results reported in this paper the following conclusions can be drawn:

(i) The 1,3-dipolar reaction between carbon−carbon multiple bonds and nitrile oxides or nitrones takes place via in-plane aromatic transition structures. The large values of the NICS computed at the (3,+1) critical points of electron density are compatible with a ring current circulating along the molecular plane.

(69) The cavitation and dispersion terms are related to the solvent-accessible surface and are virtually constant for diastereomeric structures. See: Rastelli, A.; Gandolfi, R.; Amadè, M. S. *J. Org. Chem.* **1998**, *63*, 7425.

(70) See for example: (a) Weidner-Wells, M. A.; Fraga-Spano, S.; Turchi, I. J. *J. Org. Chem.* **1998**, *63*, 6319. (b) Magnuson, E. C.; Pranata, J. *J. Comput. Chem.* **1998**, *19*, 1759.

(71) See for example: (a) Sustman, R.; Sicking, W. *Chem. Ber.* **1987**, *120*, 1471. (b) Sustman, R.; Sicking, W. *Chem. Ber.* **1987**, *120*, 1653. (c) Rastelli, A.; Bagatti, M.; Gandolfi, R.; Burdisso, M. *J. Chem. Soc., Faraday, Trans.* **1994**, *90*, 1077 and previous references therein.

(72) (a) Chandra, A. K.; Nguyen, M. T. *J. Phys. Chem. A* **1998**, *102*, 6181. (b) Méndez, F.; Tamariz, J.; Geerlings, P. *J. Phys. Chem. A* **1998**, *102*, 6292.

(ii) Solvent effects enhance the activation barrier of the reaction and decrease its synchronicity. Thus, the more polar the solvent, the larger its activation energy and the lower its synchronicity. The negative values of the NICS computed at the ring points of the transition structures do not vary with solvent effects to a significant extent.

(iii) The regiochemistry of the reaction between nitrile oxides and substituted alkenes is not determined by the aromaticity of the possible transition structures. Favorable electrostatic interactions between atoms or groups can stabilize the more asynchronous and less aromatic transition structure.

(iv) Solvent effects can determine the regiochemistry of the reaction between nitrones and substituted alkenes. The polarization of the solute must be taken into account to predict the sense of regiocontrol of the reaction. In these reactions a significant preference for endo cycloadducts is predicted, both in the gas phase and in solution.

Acknowledgment. Dedicated to Rolf Huisgen on his 80th birthday. The work in San Sebastián-Donostia was supported by the Secretaría de Estado, Investigación y Desarrollo (Project PB96-1481) and by the Gobierno Vasco-Eusko Jaurlaritza (Project EX-1997-107). A grant from the Gobierno Vasco-Eusko Jaurlaritza to I.M. is gratefully acknowledged. The work in Erlangen was supported by the Deutsche Forschungsgemeinschaft and the Fonds der Chemischen Industrie.

Supporting Information Available: Figures including drawings of products **3aa**−**3bb**, **3bd,** and **3′bd**; figures including plots of activation energies against the Onsager function and the synchronicity for the reaction between **1b** and **2b** to yield **3bb**; and tables of absolute energies and ZPVEs of all the stationary points discussed in the text and numerical data used in the elaboration of Figures S2, S3, 6, and 8 (PDF). This material is available free of charge via the Internet at http://pubs.acs.org.

JA9831397